# Modeling of Electrical Activation Ratios of Phosphorus and Nitrogen Doped Silicon Carbide

Vito Šimonka*, Andreas Hössinger‡, Josef Weinbub*, and Siegfried Selberherr†
*Christian Doppler Laboratory for High Performance TCAD at the
†Institute for Microelectronics, TU Wien, Gußhausstraße 27-29/E360, 1040 Wien, Austria
‡Silvaco Europe Ltd., Compass Point, St Ives, Cambridge, PE27 5JL, United Kingdom
Email: simonka@iue.tuwien.ac.at

***Abstract*—We propose an empirical model to accurately predict electrical activation ratios of phosphorus and nitrogen implanted silicon carbide for arbitrary annealing temperatures. We introduce model parameters and compare the activation behaviour of the two donor-type dopants. Our investigations show that the activation ratio of the nitrogen implanted silicon carbide is similar to a step function, while the activation ratio for the phosphorus implanted silicon carbide increases continuously with post-implantation annealing temperature. The model has been implemented into Silvaco's Victory Process simulator, which has enabled accurate predictions of dopant activation in post-implantation steps for silicon carbide-based processes. Several simulations have been performed to extract the depth profiles of the active dopant concentrations and to predict the activation as a function of total doping concentration and annealing temperature.**

## I. Introduction

Semiconductor devices based on silicon carbide (SiC) are typically doped by ion implantation processes followed by thermal annealing steps. This is performed in order to repair the lattice damage caused by the implantation bombardment [1] and to electrically activate the implanted impurities [2]. The post-implantation steps are therefore key to a successful device fabrication and cannot be avoided [3]. However, in order to reach the full potential of electronic devices and at the same time minimize production and operation costs, the accuracy of the process simulations is essential [4].

In recent years, SiC has shown high potential for power device applications due to its outstanding properties, i.e., wide band gap, high breakdown field, and high saturation electron drift velocity [5]. Among various SiC polytypes, 4H-SiC has the largest band gap (3.2 eV) and the highest carrier mobility ($800\ \mathrm{cm^2/Vs}$ and $115\ \mathrm{cm^2/Vs}$ for electrons and holes, respectively), therefore, it is the most attractive material [6] and thus the focus of this study.

Phosphorus (P) and nitrogen (N) are widely used shallow donor species in SiC [7]. Introducing impurities in semiconductors is used to realize free additional electrons in the conduction band. However, impurities introduce new energy levels in the band gap affecting the band structure which may significantly alter the electronic properties [8]. For this reason, it is crucial for SiC process simulations to accurately predict the effects and consequences of implantation and annealing steps.

In this work we propose an analytic model to describe the relationship between the electrical activation ratio of P and N impurities and the annealing temperature after room temperature ion implantation. Based on this theoretical approach we are able to predict the activation ratio for an arbitrary annealing temperature of either P- or N-doped SiC. The model avoids computationally expensive numerical calculations, thereby significantly improving the overall simulation speed, whilst simultaneously providing a highly accurate approximation. The proposed model is an important step to enhance the process simulation capabilities for SiC technology and has been thus embedded as an extension to the semi-empirical activation model of Silvaco's Victory Process simulator [9].

## II. Model

The major assumption of the model is that the time of the annealing processes is a minimum of 30 minutes, which assures that the doped material reaches a full activation state for the corresponding annealing temperature. The proposed model characterizes the electrical activation ratio $R$ as a function of the annealing temperature $T_\mathrm{A}$ and is written as

$$\begin{aligned} R &= R_{\frac{1}{2}} + \Big(R_\mathrm{max} - R_{\frac{1}{2}}\Big) \tanh\Big(k\ (T_\mathrm{A} - T_\mathrm{ip})\Big), \\ R_{\frac{1}{2}} &= \Big(\frac{R_\mathrm{min} + R_\mathrm{max}}{2}\Big), \end{aligned} \tag{1}$$

where $k$, $R_\mathrm{min}$, $R_\mathrm{max}$, and $T_\mathrm{ip}$ are model parameters. $R_{\frac{1}{2}}$, $R_\mathrm{max}$, and $R_\mathrm{min}$ are the half-maximal, maximal, and minimal electrical activation ratios, respectively, $k$ is the slope of the step, and $T_\mathrm{ip}$ the temperature at inflection of the curve.

The proposed relation includes a dependence on the annealing temperature only. However, in combination with the semi-empirical model from the Victory Process simulator, the post-implantation steps of process simulations additionally include a dependence on the total doping concentration. Both process variables are essential in order to maximize the efficiency of SiC devices and should be therefore accurately predicted.

## III. Results and Discussion

The donor activation is in general analyzed by investigating the free carrier concentration. We have obtained and compared several experimental measurements for P- and N-implanted SiC [1, 5-9]. We have used only the data reflecting identical SiC polytypes, orientations, and processing techniques, in



© 2017 The Japan Society of Applied Physics 

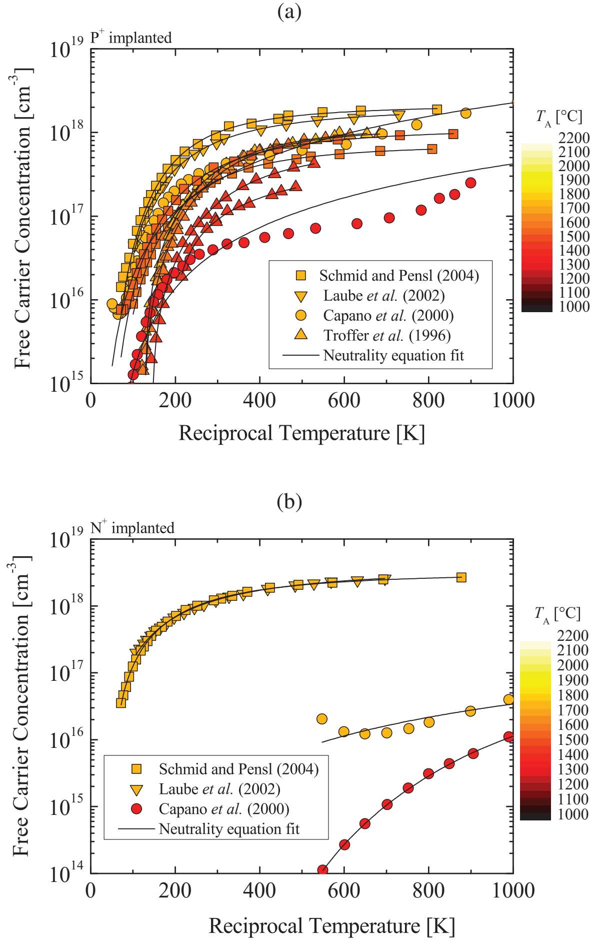


Fig. 1: Free carrier concentration as a function of reciprocal temperature for **a)** P and **b)** N-implanted SiC. Symbols refer to various experimental data, solid lines are the neutrality equation fits by this study, and colors represent various annealing temperatures.

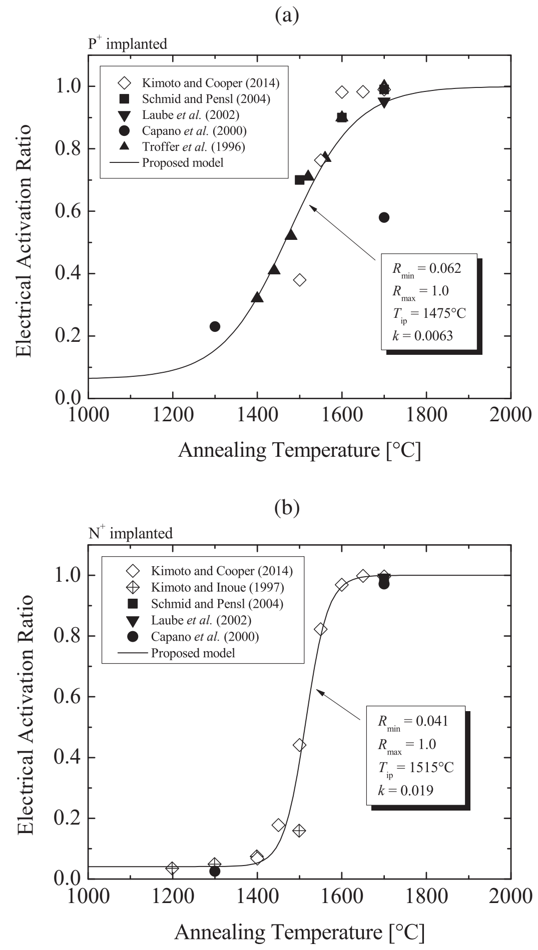


Fig. 2: Electrical activation ratio of **a)** P and **b)** N donors as a function of annealing temperature. Open symbols refer to experimental data sets, closed symbols are results from Fig. 1, and solid lines show the fit with the proposed model (1).

order to ensure investigation of annealing temperature effects only. Fig. 1 shows the collection of the free carrier concentrations as a function of the reciprocal temperature $T$ for various annealing temperatures $T_A$. In order to obtain the donor concentration $N_D$, we have fitted experimental data with the charge neutrality equation [15]:

$$n = \frac{N_D}{1 + \left(g\frac{n}{N_C}\right)\exp\left(\frac{E_i}{k_B T}\right)} - N_A$$
$$N_C = 2M_C\left(\frac{2\pi m_e k_B T}{h^2}\right)^{3/2} \quad (2)$$

$n$ is the free carrier concentration, $N_A$ the compensation acceptor concentration, $g$ the degeneracy factor, $E_i$ the ionization energy, $k_B$ the Boltzmann constant, $N_C$ the conduction band effective density of states, $M_C$ the conduction band minima, $m_e$ the effective electron mass, and $h$ the Planck constant. The parameters used for the fitting are shown in Table I.

TABLE I: Parameters for the neutrality equation fit. $m_0$ is the rest mass of an electron.

| Parameter | Value | Reference |
|---|---|---|
| $g_D$(N) | 2 | [12] |
| $g_D$(P) | 4 | [12] |
| $M_C$ | 3 | [16] |
| $m_e$ | $0.78m_0$ | [17] |

TABLE II: Model parameters for P and N doped SiC.

| Dopant | $R_{min}$ | $R_{max}$ | $Tip$ | $k$ |
|---|---|---|---|---|
| P | 0.062 | 1.0 | 1475°C | 0.0063 |
| N | 0.041 | 1.0 | 1515°C | 0.019 |

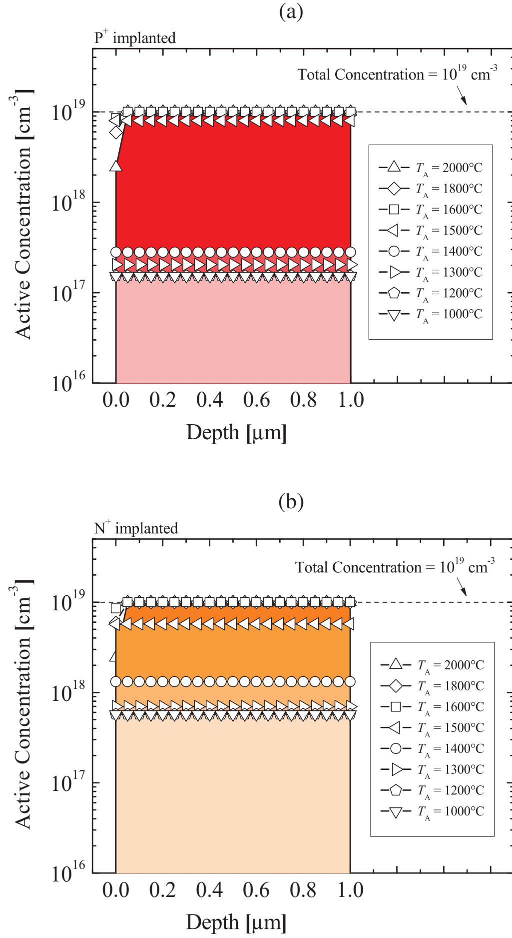


Fig. 3: Active concentration of **a)** P and **b)** N dopants in SiC for various annealing temperatures. A uniform doping profile was chosen in order to minimize diffusion effects. Simulations of implantation and annealing were performed with the Victory Process simulator. Symbols refer to various annealing temperatures.

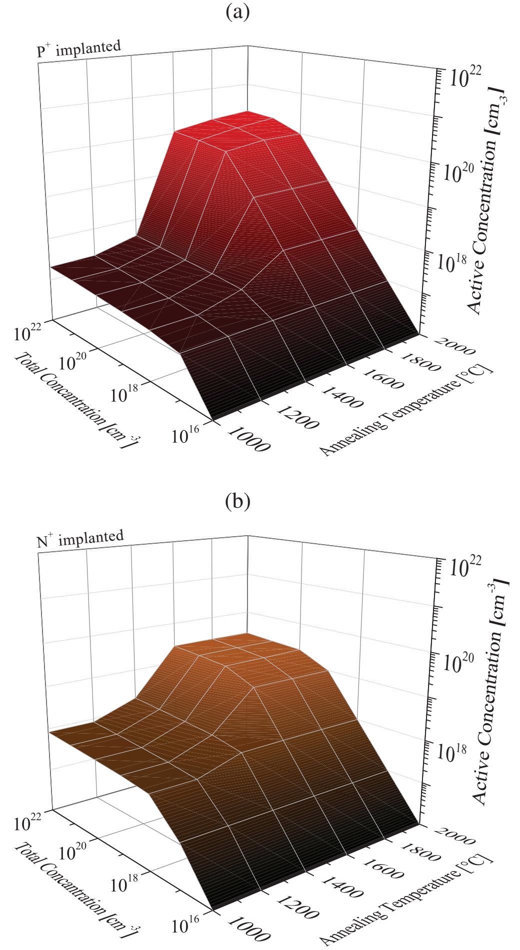


Fig. 4: Model predictions of active concentration of **a)** P and **b)** N dopants in SiC as a function of the total doping concentration and annealing temperature.

We have calculated the electrical activation ratios for various annealing temperatures as follows:

$$R = \frac{N_D}{C_x} \tag{3}$$

$C_x$ is the total P or N concentration. Fig. 2 shows the obtained activation ratios as a function of the annealing temperature. Open symbols refer to the ratios from the references in [5, 18] and closed symbols are the ratios calculated in this study. We have fitted activation ratio data sets for P and N dopants with the proposed empirical model (1), shown with solid lines. The obtained model parameters are shown in Table II.

The model suggests that P and N species reach full activation at high temperatures $T_A > 1700°C$ and that the minimal activation of both donor type dopants is approximately 5%. Additionally, the model shows that the ratio of the N implanted SiC is similar to a step function, while the ratio for the P implanted SiC increases continuously with temperature, i.e., $k(N) \approx 3k(P)$.

We have implemented the activation ratios into the Victory Process simulator's open material database and performed numerous simulations using the semi-empirical activation model. The depth profiles of the active concentrations for P and N doped SiC are shown in Fig 3. The two simulation setups are identical in order to investigate the differences between the two donor-type dopants. The total concentration of P and N impurities in SiC is $10^{19}$ cm$^{-3}$. We have achieved uniform doping profiles with several implantation steps using the available doping methods from the Victory Process simulator. The annealing steps were then performed with various annealing temperatures for each sample individually.

For both dopants we have achieved full activation for the annealing steps above $T_A = 1600°C$ and we observed no annealing effects below $T_A = 1200°C$. The main difference

between P and N impurities is detected for annealing temperatures ranging from 1400°C to 1500°C, where we observe a 10- and 5-times increase in active concentration of P and N dopants, respectively. This suggests that P impurities are activated approximately two-times more effectively in this particular temperature region.

Finally, we have investigated the correlation between the total and active concentration of donor-type SiC impurities. Fig. 4 shows the three-dimensional plot of the active dopant concentration as a function of the total doping concentration and annealing temperature for P- and N-implanted SiC. These plots are an essential model prediction, which suggested several differences between P- and N-implanted SiC. The relation between the total and active concentration is linear for $C_{tot} < 10^{17}$ cm$^{-3}$ for P- and $C_{tot} < 10^{18}$ cm$^{-3}$ for N-implanted SiC, regardless of the annealing temperature. However, above these values the relation is not trivial and is dopant, polytype, and orientation specific. Therefore, it is essential that the donor concentrations are correctly predicted by the given model.

Furthermore, we have observed that at high annealing temperatures the P donors reach a higher maximal active concentration, compared to the N donors. The maximal speed of the activation, i.e., the slope of the plot which results from the annealing temperature, is again higher for the P donors. These model results could be associated with the atomic mass of the dopant atoms and are consistent with the conclusions of Laube *et al.* [12].

## IV. Conclusions

We have proposed a model to characterize the ratio of electrical activation of P and N dopants in SiC with respect to the annealing temperature. The model enables accurate predictions of the electrical activation ratios for the annealing steps including variable temperature techniques.

Model predictions have been compared to various experimental data in order to evaluate the proposed model. We have thus been able to provide calibrated model parameters for P and N dopants in SiC. Temperature-dependent ratios were implemented into the Victory Process simulator and numerous process simulations were performed. We have shown depth profiles of the active concentration of dopants and discussed differences between two donor-type impurities.

In addition, we have investigated the influence of the total doping concentration on the activation effects. For total dopant concentrations below $\approx 10^{19}$ cm$^{-3}$ the active concentration of P and N impurities is comparable, but on the other hand, for concentrations above $\approx 10^{19}$ cm$^{-3}$, implanted P impurities reach a higher electrical activation. These model results are consistent with experimental findings [12].

Another crucial aspect of the electrical activation mechanism is a time-dependent investigation. In this study we have assumed a long annealing time to ensure maximal activation for the whole investigated temperature region. However, for various annealing temperatures the time to achieve maximal activation can vary. Therefore, to further optimize the SiC processing workflow, it is essential to predict a minimal required time to achieve full activation of the dopants for the particular annealing temperature.

## Acknowledgment

The financial support by the *Austrian Federal Ministry of Science, Research and Economy* and the *National Foundation for Research, Technology and Development* is gratefully acknowledged.

## References

[1] C. A. Fisher, R. Esteve, S. Doering, M. Roesner, M. de Biasio, M. Kraft, W. Schustereder, and R. Rupp, "An Electrical and Physical Study of Crystal Damage in High-Dose Al-and N-implanted 4H-SiC," in *Materials Science Forum*, vol. 897, 2017, pp. 411–414.

[2] R. Nipoti, A. Parisini, G. Sozzi, M. Puzzanghera, A. Parisini, and A. Carnera, "Structural and Functional Characterizations of $Al^+$ Implanted 4H-SiC Layers and $Al^+$ Implanted 4H-SiC pn Junctions after 1950 C Post Implantation Annealing," *ECS Journal of Solid State Science and Technology*, vol. 5, no. 10, pp. P621–P626, 2016.

[3] P. Fedeli, M. Gorni, A. Carnera, A. Parisini, G. Alfieri, U. Grossner, and R. Nipoti, "1950 C Post Implantation Annealing of $Al^+$ Implanted 4H-SiC: Relevance of the Annealing Time," *ECS Journal of Solid State Science and Technology*, vol. 5, no. 9, pp. P534–P539, 2016.

[4] V. Borisenko and P. J. Hesketh, *Rapid Thermal Processing of Semiconductors*. Springer, 2013.

[5] T. Kimoto and J. A. Cooper, *Fundamentals of Silicon Carbide Technology: Growth, Characterization, Devices and Applications*. John Wiley & Sons, 2014.

[6] Y. Hijikata, *Physics and Technology of Silicon Carbide Devices*. InTech, 2013.

[7] W. J. Choyke, H. Matsunami, and G. Pensl, *Silicon Carbide: Recent Major Advances*. Springer Science & Business Media, 2013.

[8] P. T. Landsberg, *Basic Properties of Semiconductors*. Elsevier, 2016.

[9] http://www.silvaco.com/products/tcad/.

[10] T. Kimoto and N. Inoue, "Nitrogen Ion Implantation into $\alpha$-SiC Epitaxial Layers," *Physica Status Solidi (a)*, vol. 162, no. 1, pp. 263–276, 1997.

[11] F. Schmid and G. Pensl, "Comparison of the Electrical Activation of $P^+$ and $N^+$ Ions Co-Implanted Along with $Si^+$ or $C^+$ Ions into 4H-SiC," *Applied Physics Letters*, vol. 84, no. 16, pp. 3064–3066, 2004.

[12] M. Laube, F. Schmid, G. Pensl, G. Wagner, M. Linnarsson, and M. Maier, "Electrical Activation of High Concentrations of $N^+$ and $P^+$ Ions Implanted Into 4H-SiC," *Journal of Applied Physics*, vol. 92, no. 1, pp. 549–554, 2002.

[13] M. A. Capano, J. Cooper Jr, M. Melloch, A. Saxler, and W. Mitchel, "Ionization Energies and Electron Mobilities in Phosphorus and Nitrogen-Implanted 4H-Silicon Carbide," *Journal of Applied Physics*, vol. 87, no. 12, pp. 8773–8777, 2000.

[14] T. Troffer, C. Peppermüller, G. Pensl, K. Rottner, and A. Schöner, "Phosphorus-Related Donors in 6H-SiC Generated by Ion Implantation," *Journal of Applied Physics*, vol. 80, no. 7, pp. 3739–3743, 1996.

[15] C.-M. Zetterling, *Process Technology for Silicon Carbide Devices*. IET, 2002, no. 2.

[16] F. Schmid, M. Laube, G. Pensl, G. Wagner, and M. Maier, "Electrical Activation of Implanted Phosphorus Ions in [0001] and [11-20]-Oriented 4H-SiC," *Journal of Applied Physics*, vol. 91, no. 11, pp. 9182–9186, 2002.

[17] G. Wellenhofer and U. Rössler, "Global Band Structure and Near-Band-Edge States," *Physica Status Solidi (b)*, vol. 202, no. 1, pp. 107–123, 1997.

[18] T. Kimoto, O. Takemura, H. Matsunami, T. Nakata, and M. Inoue, "$Al^+$ and $B^+$ Implantations into 6H-SiC Epilayers and Application to pn Junction Diodes," *Journal of Electronic Materials*, vol. 27, no. 4, pp. 358–364, 1998.